Pseudogap and Charge Dynamics in CuO_2 Planes in YBCO

D. N. Basov,[1,2] R. Liang,[3] B. Dabrowski,[4] D. A. Bonn,[3] W. N. Hardy,[3] and T. Timusk[1]
[1]*Department of Physics and Astronomy, McMaster University, Hamilton, Ontario, Canada L8S 4M1*
[2]*Department of Physics, Brookhaven National Laboratory, Upton, New York 11973-5000*
[3]*University of British Columbia, Vancouver, BC, Canada V6T 4M1*
[4]*Department of Physics, University of Northern Illinois, DeKalb, Illinois 60115*
(Received 4 April 1996)

We report on the infrared conductivity of $YBa_2Cu_3O_x$ and $YBa_2Cu_4O_8$ crystals with different oxygen content and Zn doping. We find a correlation between the structure of the scattering rate spectra $1/\tau_a^*(\omega,T)$ in the CuO_2 planes and the pseudogap that develops in the *c*-axis conductivity of underdoped samples for $T < T^* = 140-250$ K. In the pseudogap state, the scattering rate is depressed at low frequencies and follows an $\omega^{2\pm0.3}$ law for $\omega < 400$ cm^{-1}. When the *c*-axis pseudogap is suppressed, either by an increase of temperature above T^* or by a substitution of Cu with Zn, the spectra of $1/\tau_a^*(\omega,T)$ revert to the nearly linear ω dependence of the optimally doped compounds. [S0031-9007(96)01596-7]

PACS numbers: 78.30.Er, 74.25.Gz, 74.72.Bk,

It is now well established that the electronic properties of high-T_c cuprates are very different from those of conventional metals. In optimally doped samples (those with maximum T_c), a resistivity ρ_{dc} along the CuO_2 planes that is linear in T with a zero intercept at $T = 0$ [1] and a temperature dependent Hall coefficient [2] are indicative of strong correlations between charge carriers [3]. Effects due to correlations are also observed in materials with reduced carrier densities, commonly designated as "underdoped." The ρ_{dc} of underdoped compounds [4,5] show anomalies that occur around a characteristic temperature $T = T^* > T_c$, where nuclear magnetic resonance [6], specific heat [7], and neutron [8] experiments point to the opening of a pseudogap in the spectrum of low- energy excitations. This pseudogap can be observed directly by infrared measurements of the interplane *c*-axis conductivity of underdoped YBCO [9,10].

The purpose of this study is to investigate, by means of infrared spectroscopy, the influence that the pseudogap has on the peculiar charge dynamics of the CuO_2 planes. As a model system we have chosen YBCO. Advantages of YBCO include the availability of high quality samples and convenient access to different hole doping regimes through the oxygenation/deoxygenation of the same crystal. Also, by using detwinned crystals one can probe the response of the CuO_2 planes without having to consider the contribution to the optical conductivity from charge reservoir layers. In other cuprates, the reservoir layers (Tl-O, Bi-O, etc.) inevitably contribute to the planar conductivity. However, in YBCO the reservoir is in the one-dimensional Cu-O chain, so the response to the E vector perpendicular to the chain direction ($E \parallel a$), as measured in untwinned crystals, is determined solely by the CuO_2 planes.

In this Letter we present, for the first time, a complete set of data illustrating the evolution of the in- and interplane conductivity of a high-T_c superconductor with changes in carrier density, temperature, and disorder of the CuO_2 planes through the substitution of Zn for Cu. We find a link between lifetime effects in the CuO_2 planes and the pseudogap in the *c*-axis conductivity. The complex conductivity $\sigma_1(\omega) + i\sigma_2(\omega)$ of YBCO single crystals was obtained from Kramers-Kronig analysis of the reflectance measured for polarizations $E \parallel a$ and $E \parallel c$ between 30–50 cm^{-1} and 20 000 cm^{-1}. Three regimes of carrier density were studied: a mechanically detwinned optimally doped $YBa_2Cu_3O_x$ (123) crystal with oxygen content set at $x = 6.95$ ($T_c = 93.5$ K), the same crystal deoxygenated down to $x = 6.6$ ($T_c = 59$ K) [11], and a double-chained $YBa_2Cu_4O_8$ (124) crystal with $T_c = 82$ K [12]. The carrier density in naturally untwinned 124 crystal corresponded to that of 123 samples with $x \simeq 6.85$. We also studied a series of 124 crystals where Cu ions in the CuO_2 planes were substituted with Zn [13].

In Fig. 1, the real part of the in-plane conductivity $\sigma_a(\omega)$ of the YBCO crystals is plotted together with earlier data for the real part of the *c*-axis conductivity $\sigma_c(\omega)$ [9,10,14]. The in-plane response of all samples is Drude-like, i.e., the absolute value of $\sigma_a(\omega)$ decreases from the dc value with increasing ω. The in-plane plasma frequency $\omega_p = [8\int_0^\infty \sigma_a(\omega)\,d\omega]^{1/2}$, scales with T_c in accordance with with previous work [15].

The frequency dependence of the $\sigma_a(\omega)$ spectra change with doping: particularly the width of the Drude-like peak at $T \simeq T_c$ narrows with decreasing carrier density. To accentuate these differences we plot the spectra of the renormalized in-plane scattering rate in the form $1/\tau_a^*(\omega,T)$, which we obtain from an extended Drude model [16]:

$$\frac{1}{\tau_a^*(\omega,T)} = \omega\frac{\sigma_1(\omega,T)}{\sigma_2(\omega,T)}. \qquad (1)$$

For cuprates, $1/\tau_a^*(\omega,T)$ is often frequency dependent [15,17]. The cause of this frequency dependence is believed to be inelastic scattering of quasiparticles by

 0031-9007/96/77(19)/4090(4)$10.00

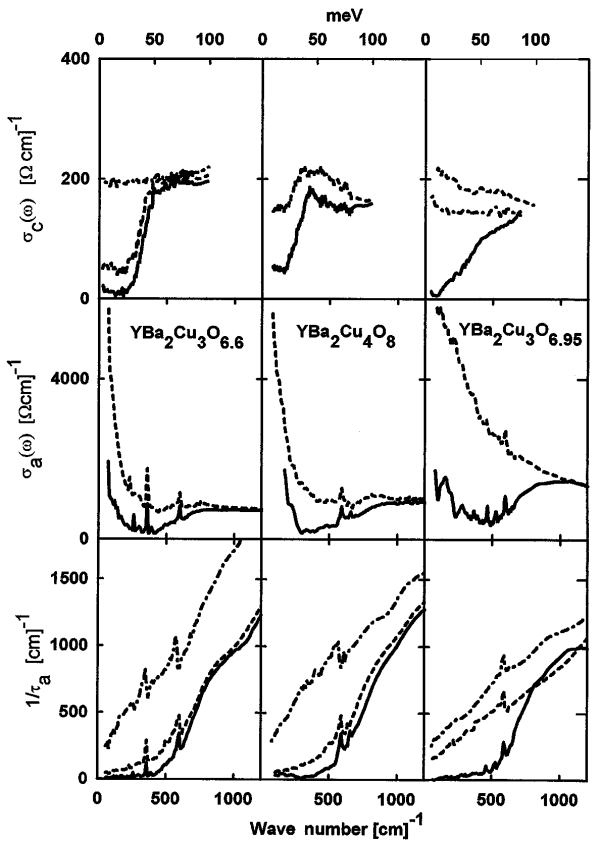

FIG. 1. The c-axis conductivity (top panel), the a-axis conductivity (middle panel), and the a-axis scattering rate Eq. (1) (bottom panel) of $YBa_2Cu_3O_{6.95}$, ($T_c = 93.5$ K), $YBa_2Cu_3O_{6.6}$ ($T_c = 59$ K), and of $YBa_2Cu_4O_8$ ($T_c = 82$ K) single crystals. Dash-dotted lines—$T = 300$ K, dashed lines $T \simeq T_c$, solid lines at $T = 10$ K. The c-axis conductivity of 123 crystals is taken from Ref. [10] and multiplied by a factor of 4; the c-axis conductity of 124 crystals is from Ref. [11]. Upon opening of a pseudogap in the c-axis conductivity (at $T < T^*$ in underdoped 123 and 124) the in-plane transport is altered as well and the Drude-like feature in $\sigma_a(\omega)$ is narrowing. That corresponds to a depressed scattering rate at low frequencies and leads to a threshold feature in the spectra of $1/\tau_a^*(\omega, T)$. When the psedogap in $\sigma_c(\omega)$ is not observed (at $T < T^*$ in the underdoped 123 and 124 or at $T > T_c$ in the optimally doped 123) the in-plane $a/\tau_a^*(\omega, T)$ shows nearly linear dependence consistent with the gapless scattering spectrum.

excitations possessing a broad energy spectrum, $F(\omega)$ [18]. These inelastic processes are mirrored in the ω dependence of $1/\tau_a^*(\omega, T)$, which reflects the energy scales associated with the $F(\omega)$ spectrum [19,20].

In an optimally doped crystal $1/\tau_a^*(\omega, T)$ is a linear function of both energy and temperature. The absolute value is of the order of ω, which is consistent with strong scattering from a flat $F(\omega)$ spectrum [18]. As the temperature decreases from 300 K to T_c the spectra of $1/\tau_a^*(\omega, T)$ shift down by an amount proportional to kT without any significant changes to the frequency dependence. Thus the scattering rate can be written as a sum of three terms:

$$\frac{1}{\tau_a^*(\omega, T)} = \frac{1}{\tau_0} + \frac{1}{\tau(T)} + \frac{1}{\tau(\omega)}, \qquad (2)$$

where the first term stands for impurity scattering, the second and the third terms for the ω and T dependence, respectively. This behavior should be contrasted with the standard Fermi liquid picture where the quasiparticle damping $\hbar/\tau$ is supposed to be much lower than their energy, and vary quadratically with T and ω [21].

In the underdoped samples the situation is even more complex. In agreement with the earlier data [15], our 300 K scattering rates for the 123 $x = 6.6$ crystal and the 124 sample still exhibit nearly linear frequency dependence. However, unlike the case of the optimally doped sample, the temperature dependence of $1/\tau_a^*(\omega, T)$ in the underdoped 123 and 124 is not restricted just to a vertical offset of the spectra. Rather than being a simple offset, one finds a *change* in the ω dependence of the in-plane scattering rate for temperatures $T < T^*$, which is about 140 K for the 124 crystals and about 250 K for the 123 $x = 6.6$ sample. For temperatures below T^*, $1/\tau_a^*(\omega, T)$ develops a threshold feature at $\omega \simeq 600$ cm^{-1}. As a result of this threshold, the temperature dependence of $1/\tau_a^*(\omega \to 0, T)$ falls *faster* than linearly. This is in accord with measurements of the dc resistivity $\rho(T)$ that indicate a crossover to a steeper slope in $d\rho/dT$ below T^* in the underdoped crystals [4,22].

The c-axis response of underdoped crystals is modified below T^* as well. Both 123 $x = 6.6$ and 124 reveal a *pseudogap* in the FIR conductivity—a region where $\sigma_c(\omega)$ is reduced but remains finite [9,10]. The formation of the pseudogap in $\sigma_c(\omega)$ occurs through the transfer of spectral weight from FIR frequencies ($\omega < 300$ cm^{-1}) to higher energies. Thus the suppression of the scattering rate within the CuO_2 planes is accompanied by a redistribution of the c-axis spectral weight. We emphasize that the spectral weight in the a-axis conductivity shows no transfer to higher energy in the same temperature range.

To further explore the connection between the in-plane scattering rate and the c-axis pseudogap we studied 124 crystals doped with Zn. In Fig. 2 we plot the spectra of $\sigma_a(\omega)$, $\sigma_c(\omega)$, and $1/\tau_a^*(\omega, T)$ of 124 samples of $YBa_2(Cu_{1-y}Zn_y)_4O_8$, where $y = 0.004\,25$. As a result of this substitution T_c is suppressed from 82 K in the pure crystal down to 45 K [23]. Substitution with Zn also leads to an increase of $1/\tau_0$ by 110–130 cm^{-1} and a radical alteration of the frequency dependence of $1/\tau_a^*(\omega)$ and $\sigma_a(\omega)$. The threshold structure in the in-plane scattering rate nearly vanishes in the crystal containing Zn. The c-axis results obtained for this sample also reveal a *complete suppression* of the pseudogap [25]. The overall result is that the in-plane and c-axis properties of this *underdoped* system with Zn impurities at $T > T_c$ are quite similar to the *optimally doped* 123 sample with $x = 6.95$.

The results presented in Figs. 1 and 2 establish a correlation between the c-axis pseudogap and the gaplike structure in the in-plane scattering rate. First, the threshold

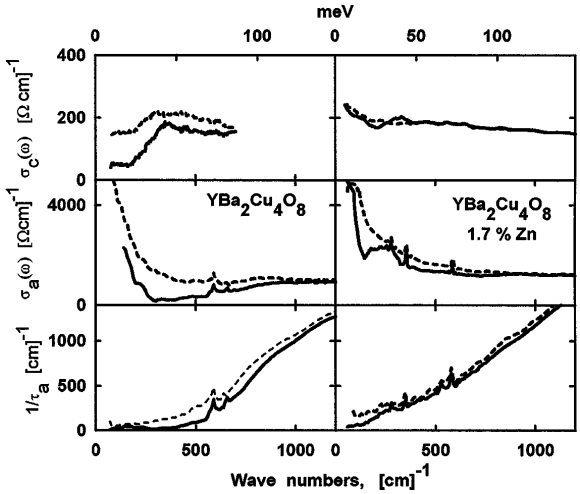

FIG. 2. The c-axis conductivity (top panel), the a-axis conductivity (middle panel), and the a-axis scattering rate [obtained from Eq. (1)] (bottom panel) of a pure 124 crystal and of $YBa_2(Cu_{1-x}Zn_x)_4O_8$ ($x = 0.0045$, $T_c = 45$ K) crystals. Dashed lines $T \simeq T_c$, solid lines at $T = 10$ K. The pseudo gap in $\sigma_c(\omega)$ and a threshold structure in $1/\tau_a^*(\omega, T)$ are found only in "clean" 124 crystals. A substitution of Cu with Zn in this *underdoped* crystal suppresses the pseudogap in the c-axis conductinty and restores nearly linear behavior of $1/\tau_a^*(\omega, T)$ originally found in the *optimally doped* 123 crystal.

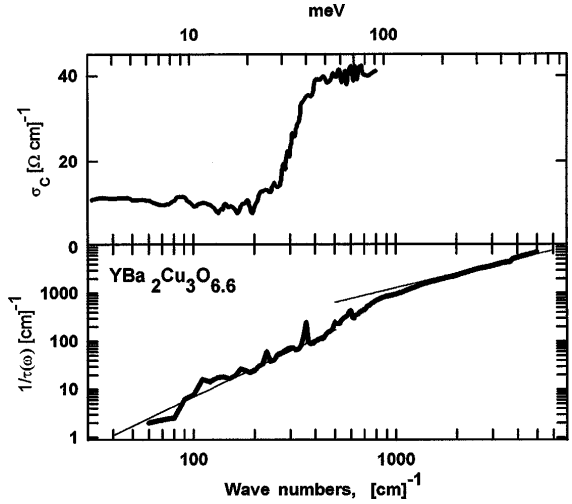

FIG. 3. Top panel—the c-axis conductivity of underdoped 123 crystal from Ref. [10]. Bottom panel—the frequency dependent term on the right-hand side of Eq. (2) [$1/\tau(\omega)$] obtained from $1/\tau_a^*(\omega, T)$ as described in the text for $YBa_2Cu_3O_{6.6}$. The spectrum of $1/\tau(\omega)$ shows a crossover from a strong scattering regime at $\omega > 1500$ cm^{-1}, where $1/\tau(\omega) \simeq \omega$ and varies linearly with frequency to weak scattering regime at $\omega < 400$ cm^{-1}, where $1/\tau(\omega) < \omega$ and varies quadratically with frequency. The crossover region matches the position of the steplike structure in $\sigma_c(\omega)$. Thin solid lines show ω^1 and $\omega^{2\Theta}$ dependences.

feature in $1/\tau_a^*(\omega, T)$ is found only in underdoped crystals at $T < T^*$ when the spectrum of $\sigma_c(\omega)$ exhibits a pseudogap. Second, the suppression of the pseudogap in $\sigma_c(\omega)$, either by the increase of temperature above T^*, or by the increase of the carrier density from $x = 6.6$ to 6.95 in 123, or by the substitution of Cu with Zn in underdoped 124, restores the nearly linear frequency dependence of the $1/\tau_a^*(\omega)$.

In order to analyze the frequency dependent part of the scattering rate [$1/\tau(\omega)$—the third term in Eq. (2)] in underdoped crystals, we first subtract the $1/\tau(T)$ contribution from $1/\tau_a^*(\omega, T \simeq T_c)$ in Eq. (2). To estimate this contribution we assume that the value of $1/\tau_a^*(\omega, T)$ at frequencies much higher than the gaplike structure ($\omega > 2000$ cm^{-1}) is dictated primarily by the $1/\tau(T)$ term (as in the optimally doped samples). Then $1/\tau(T)$ can be obtained as $1/\tau_a^*(2000, T_c) - 1/\tau_a^* \times (2000, 10)$. This yields the value of $1/\tau(T \simeq T_c)$ which is close to kT–43 cm^{-1} for the 123 $x = 6.6$ sample and 56 cm^{-1} for the 124 sample. In Fig. 3 we show the spectrum of $1/\tau(\omega)$ for the underdoped 123 crystal at 65 K on a log-log scale. The spectrum shows a crossover from the strong scattering regime at $\omega > 1500$ cm^{-1}, where the slope is linear and $1/\tau(\omega) \simeq \omega$ to a *weak* scattering regime at $\omega < 400$ cm^{-1}, where $1/\tau(\omega) < \omega$ and varies as $\omega^{2\pm0.3}$. This behavior is in accord with that of the dc resistivity which shows a nearly quadratic dependence of $\rho(T)$ below 200 K [22]. Remarkably, the weak scattering regime is observed in a frequency range which coincides with the pseudogap in the c-axis conductivity and there is a crossover to strong in-plane scattering at frequencies exceeding the steplike structure in $\sigma_c(\omega)$. All of the above observations hold true for the 124 sample as well.

Below, we summarize the principal conclusions that follow from Figs. 1–3. (i) In order to be consistent with the experimental behavior of $1/\tau_a^*(\omega, T)$ the spectrum $F(\omega)$ of excitations responsible for the scattering in the CuO_2 planes has to be suppressed at low frequencies in the same temperature range and in the same doping regime where the c-axis conductivity reveals a pseudogap. (ii) A crossover to stronger in-plane scattering in underdoped 123 and in 124 starts when the frequency exceeds the magnitude of the c-axis pseudogap. This suggests that for underdoped crystals the c-axis conductivity reproduces certain features of the in-plane scattering spectrum, $F(\omega)$. (iii) The development of a threshold feature in the spectra of $1/\tau_a^*(\omega, T)$ at $T < T^*$ and its suppression with addition of Zn impurities argues in favor of the scattering excitations being related to the *spin* degree of freedom. (iv) In the pseudogap state the in-plane transport of YBCO mimics certain features of a Fermi liquid by showing a nearly quadratic ω dependence of $1/\tau_a^*(\omega)$. However, this behavior is found only in the regime where the c-axis properties such as semiconducting resistivity and the presence of a pseudogap in the spectra of $\sigma_c(\omega)$ basically rule out a standard Fermi liquid approach to data interpretation.

Finally, we discuss the response at $T < T_c$. A brief examination of the data presented in Fig. 1 shows that the electrodynamic properties in underdoped crystals undergo qualitative changes at $T < T^*$ but are very similar in the pseudogap state and in the superconducting state. This is

true for both the in-plane and interplane properties. The frequency dependence of the c-axis conductivity of 123 $x = 6.6$ and of 124 crystals is essentially the same at $T \simeq T_c < T^*$ and at 10 K. The in-plane charge dynamics of underdoped samples also changes very little at T_c. The principal feature of the $1/\tau_a^*(\omega)$ spectra is a gaplike threshold which appears at $T < T^*$, and there are almost no differences between the spectra obtained at 10 K and at $T \simeq T_c < T^*$.

Results presented in Fig. 1 clearly show that the electrodynamics of underdoped crystals are determined by *two* characteristics temperatures: T^* and T_c. We regard these observations as truly extraordinary, for it is well established that superconductivity of simple metals involves only one energy scale set by T_c. Above T_c elemental superconductors are undistinguishable from normal metals. However, in underdoped YBCO the charge dynamics is altered at $T^* > T_c$ and no qualitative changes are seen when the sample becomes superconducting.

With increased doping, T^* is suppressed whereas T_c increases. Thus the phase region representing the pseudogap state in the T versus doping level diagram would gradually be reduced. We suggest that in optimally doped crystals the T^* and T_c coincide. In accord with this view the 10 K scattering rate spectrum of the 123 $x = 6.95$ crystal shows a frequency dependence which is remarkably similar to the data obtained for underdoped samples in the pseudogap state [27]. Phase diagrams with the pseudogap region have recently been predicted within two different theoretical frameworks: spin-charge separation and phase fluctuations [28,29]. Each of these models could provide its own scenario for a causal connection between lifetime effects in the CuO_2 plane and a pseudogap in the interplane conductivity. We are looking forward to a comparison of our experimental data with the results of detailed theoretical analysis of the ω and T dependence of the electromagnetic response in various doping and impurity regimes. Such a comparison may help to distinguish between the proposed models or perhaps indicate a certain degree of convergence between these ideas.

The authors acknowledge illuminating discussions with A. J. Berlinsky, J. Carbotte, V. Emery, C. C. Homes, M. Julien, P. A. Lee, K. Kallin, S. Kivelson, D. Pines, A. V. Puchkov, and Y. Uemura. This work was supported by the CIAR and the NSERC (D. N. B., R. L., D. A. B., W. N. H, and T. T), U.S. DOE under Contract No. DE-AC02-76CM00016 (D. N. B.) and by U.S. DOE under Contract No. DE-AC05-84OR21400 (B. D.).

[1] M. Gurvitch and A. T. Fliory, Phys. Rev. Lett. **59**, 1337 (1987).
[2] H. L. Stromer *et al.*, Phys. Rev. B **38**, 2472 (1988).
[3] P. W. Anderson, Science **235**, 1196 (1987).
[4] B. Bucher *et al.*, Phys. Rev. Lett. **70**, 2012 (1993).
[5] B. Batlogg *et al.*, Physica (Amsterdam) **235C–240C**, 130 (1994).
[6] M. Takigawa *et al.*, Phys. Rev. B **43**, 247 (1991).
[7] J. W. Loram *et al.*, Phys. Rev. Lett. **71**, 1740 (1993).
[8] J. M. Tranquada *et al.*, Phys. Rev. B **46**, 5561 (1992).
[9] C. C. Homes *et al.*, Phys. Rev. Lett. **71**, 1645 (1993); C. C. Homes *et al.*, Physica (Amsterdam) **254C**, 265 (1995).
[10] D. N. Basov *et al.*, Phys. Rev. B **50**, 3511 (1994); D. N. Basov *et al.*, Phys. Rev. B **52**, R13 141 (1995).
[11] Ruxiang Liang *et al.* Physica (Amsterdam) **195C**, 51 (1992).
[12] B. Dabrowski *et al.*, Physica (Amsterdam) **202C**, 271 (1992).
[13] B. Dabrowski (unpublished).
[14] The interplane conductivity of YBCO and of all cuprates is dominated by a series of infrared-active phonons which were removed from the $\sigma_c(\omega)$ spectra shown in Fig. 1 by fitting them with Lorentzian oscillators (see Refs. [10,11]). The phonon features in the $\sigma_a(\omega)$ and in $1/\tau_a(\omega)$ have not been removed and give sharp peaks in these spectra at $300 < \omega < 600$ cm^{-1}.
[15] J. Orenstein *et al.*, Phys. Rev. B **42**, 6342 (1990); L. D. Rotter *et al.*, Phys. Rev. Lett. **67**, 2741 (1991); S. L. Cooper *et al.*, Phys. Rev. B **47**, 8233 (1993).
[16] J. W. Allen and J. C. Mikkelsen, Phys. Rev. B **15**, 2952 (1977).
[17] B. Bucher *et al.*,, Phys. Rev. B **45**, 3026 (1992).
[18] P. B. Littlewood and C. M. Varma, J. Appl. Phys. **69**, 4979 (1991); Phys. Rev. B **46**, 405 (1992).
[19] R. R. Joyce and P. L. Richards, Phys. Rev. Lett. **24**, 1007 (1970).
[20] P. B. Allen, Phys. Rev. B **3**, 305 (1971).
[21] D. Pines and P. Nozieres, *The Theory of Quantum Liquids* (Benjamin, New York, 1966).
[22] K. Takenaka *et al.*, Phys. Rev. B **50**, 6534 (1994).
[23] While a detailed structural study of Zn doping in the 124 system has not been performed, it has been shown in Ref. [24] that in the 123 compound Zn predominantly occupies Cu sites in the CuO_2 planes.
[24] G. Xiao *et al.*, Nature (London) **332**, 238 (1988).
[25] The effect of Zn on the c-axis pseudogap is similar to the one observed in the spin-lattice relaxation time $1/TT_1$ [26]. A similar concentration of Zn in ceramic pellets of 124 completely suppresses the pseudogap feature in the temperature dependence of $1/TT_1$, but the behavior of the Knight shift remains unchanged from that of a pure sample.
[26] G. Zheng *et al.*, J. Phys. Soc. Jpn. **62**, 2591 (1993).
[27] In this Letter we do not attempt to perform an analysis of the frequency dependence of the scattering rate in the superconducting state. This is because such an analysis requires a complicated procedure to account for an additional decrease of $\sigma_1(\omega)/\sigma_2(\omega)$ in Eq. (1) resulting from the formation of the superconducting condensate.
[28] N. Nagaosa and P. A. Lee, Phys. Rev. Lett. **64**, 2450 (1990).
[29] V. J. Emery and S. A. Kivelson, Nature (London) **374**, 434 (1995).